

Spin-Polarized Radicals with Extremely Long Spin-Lattice Relaxation Time at Room Temperature in a Metal-Organic Framework

Kana Orihashi,^a Akio Yamauchi,^a Saiya Fujiwara,^b Mizue Asada,^c Toshikazu Nakamura,^c Joseph Ka-Ho Hui,^a Nobuo Kimizuka,^a Kenichiro Tateishi,^d Tomohiro Uesaka,^d and Nobuhiro Yanai*^{a,e}

^aDepartment of Applied Chemistry, Graduate School of Engineering and Center for Molecular Systems (CMS), Kyushu University, 744 Moto-oka, Nishi-ku, Fukuoka 819-0395, Japan.

^bRIKEN Center for Emergent Matter Science, Riken, Wako, Saitama 351-0198, Japan.

^cInstitute for Molecular Science, Nishigonaka 38, Myodaiji, Okazaki 444-8585, Japan

^dCluster for Pioneering Research, Nishina Center for Accelerator-Based Science, RIKEN, 2-1 Hirosawa, Wako, Saitama 351-0198, Japan).

^eFOREST, JST, Honcho 4-1-8, Kawaguchi, Saitama 332-0012, Japan.

ABSTRACT: The generation of spin polarization is key in quantum information science and dynamical nuclear polarization. Polarized electron spins with long spin-lattice relaxation times (T_1) at room temperature are important for these applications, but have been difficult to achieve. We report the realization of spin-polarized radicals with extremely long T_1 at room temperature in a metal-organic framework (MOF) in which azaacene chromophores are densely integrated. Persistent radicals are generated in the MOF by charge separation after photoexcitation. Spin polarization of triplet generated by photoexcitation are successfully transferred to the persistent radicals. Pulse ESR measurements reveal that the T_1 of the polarized radical in the MOF is as long as 274 μs at room temperature. The achievement of extremely long spin polarization in MOFs with nanopores accessible to guest molecules will be an important cornerstone for future highly sensitive quantum sensing and efficient dynamic nuclear polarization.

Generating and controlling electron spin polarization (ESP) is crucial in the foundation of a wide range of spin-related technologies. In the context of quantum information science, it provides the spin systems necessary for qubit operation and it also leads to highly sensitive quantum sensing.¹⁻³ Dynamic nuclear polarization (DNP), which transfers the polarization from electron spins to nuclear spins, can lead to increased sensitivity in nuclear magnetic resonance and magnetic resonance imaging.⁴⁻⁸ ESP using molecular materials has attracted particular attention because of their high polarization performance and atomic-scale controllability.^{9,10} A variety of molecular materials showing dynamic electron polarization have been developed, including radical pairs,¹¹ chromophore triplets,¹² chromophore radical hybrids,^{13,14} and metal complexes.^{10,15,16}

In addition to ESP, long spin-lattice relaxation times (T_1) are important for spin manipulations and highly efficient DNP.¹⁷ If ESP with a long T_1 at room temperature can be achieved, quantum sensing and DNP at the temperature where biomolecules are actually active would be realized. T_1 of polarized spins have been evaluated in various molecular materials and although those with long T_1 at cryogenic temperatures have been observed,¹⁸ T_1 near room temperature is often only a few or tens of micro-seconds.¹⁹ The development of molecular materials exhibiting ESP with a longer T_1 at room temperature will be the key to

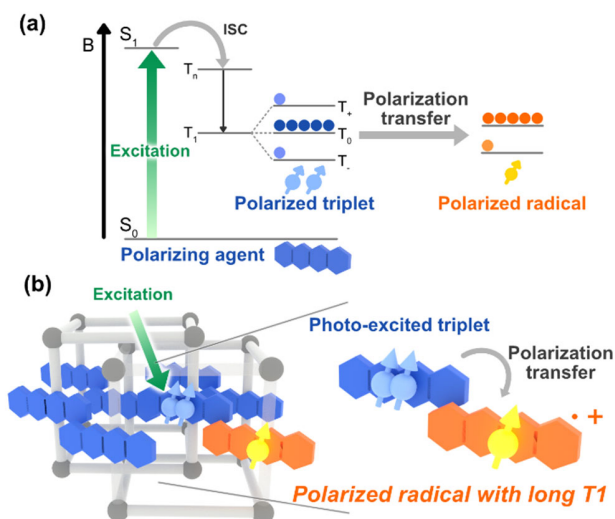


Figure 1. (a) Generation mechanism of spin-polarized radicals. Photoexcitation of the chromophore is followed by spin-selective intersystem crossing (ISC), resulted in polarized triplet excited state. Radical species originated from charge separation are hyperpolarized by receiving the polarization from the triplet state. (b) Schematic illustration of photo-induced generation of polarized triplet and subsequent polarization transfer from triplets to radicals in a chromophore-assembled metal-organic framework (MOF).

expanding the scope of future molecular quantum technology.

In this study, we report an extremely long ESP with a T_1 exceeding 270 μs at room temperature in a chromophore-integrated metal-organic framework (MOF). MOFs are crystalline network materials composed of metal ions and bridging organic ligands, and they offer an excellent platform to precisely control the arrangement of chromophore units in the ligands. Photoexcitation of the MOF generated triplet excited states and charge-separated persistent radicals. Immediately after the pulsed photo-excitation, the ESP of triplets was transferred to that of radicals, and radicals retained the ESP for several hundred microseconds (Figure 1). From pulsed electron spin resonance (ESR) measurements, the T_1 of the radicals was determined to be 274 μs at room temperature. This surprising finding demonstrates that molecular materials can indeed achieve ESP with T_1 as long as several hundred microseconds even at room temperature, and that quantum technology based on chromophore-integrated materials is a promising direction for future works.

To obtain large ESP at room temperature, it is effective to use photo-excited states of molecules. Excited triplets of organic molecules have large ESP and do not contain heavy elements, so they are less likely to suffer from severe spin relaxation. Acene compounds are typical examples of materials which produce polarized triplets. Among them, our group has shown that 5,12-diazatetracene (DAT) in which an electron-withdrawing nitrogen atom was introduced, is a high-performance polarizing agent with high stability in air and high solubility in common organic solvents which is useful for DNP applications.²⁰⁻²² In this study, a new organic ligand, 6,11-di(pyridine-4-yl)benzo[*b*]phenazine (DPyDAT, Figure 2a), was synthesized by modifying DAT with pyridine as a coordination site to the metal, and its purity was confirmed by NMR, mass spectrometry and elemental analysis (see Supporting Information for details). The solvothermal reaction of $\text{Zn}(\text{NO}_3)_2 \cdot 6\text{H}_2\text{O}$ with linkers DPyDAT and 4,4'-biphenyldicarboxylic acid (BPDC) in DMF gave MOF crystals with the formula of $[\text{Zn}_2(\text{BPDC})_2(\text{DPyDAT})]_n \cdot 1.5\text{H}_2\text{O}$ (Figure 2a). The obtained MOF is named as DAT-MOF.

Single crystal structure analysis of DAT-MOF revealed that it has a pillared-layer three-dimensional network [CCDC 2243198]. Two-dimensional sheets composed of distorted Zn paddlewheel dimers and BPDC are cross-linked by DPyDAT pillars.^{23,24} The three-dimensional network is further doubly interpenetrated (Figure 2b and S1). One benzene ring of BPDC and DAT are in parallel, and the carbon-carbon distance is relatively close around 3.5 \AA , forming π - π interactions between the three-dimensional networks. There is no π - π stacking between DAT moieties, while the core-to-core distance between the nearest DAT units is about 1 nm and the distance between the nearest carbon atoms is 0.33 nm (Figure 2c). The purity of bulk crystalline powder of DAT-MOF was confirmed by elemental analysis and the good agreement of the X-ray powder diffraction (PXRD) patterns with the simulation results obtained from the single crystal structure (Figure S2).

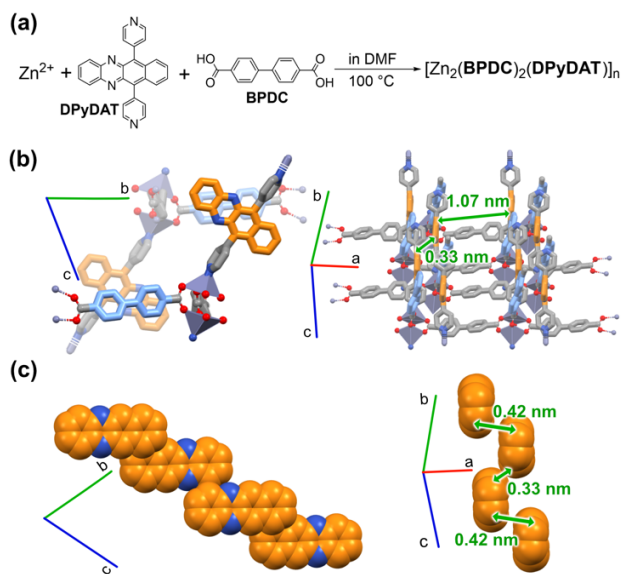


Figure 2. (a) Synthetic scheme of DAT-MOF. (b) Crystal structure of DAT-MOF. (c) The arrangement of DAT units in the DAT-MOF crystal structure.

ESP formation of DAT-MOF was evaluated by time-resolved ESR measurements (Figure 3a) using X-band (~ 9.6 GHz) at room temperature under pulsed laser excitation with a wavelength, frequency, and power of 532 nm, 30 Hz, and 2-3 mJ/pulse, respectively. To prevent damage by laser irradiation and oxygen, the DAT-MOF powder was immersed in paraffin in a capillary of 2.0 mm outer diameter, degassed, and fire-sealed. A reference sample, in which only the DPyDAT ligand was dispersed in PMMA, showed an eaeaa pattern characteristic of the DAT triplet (Figure S3), and its polarization magnitude and zero-field splitting parameters were similar to those of DAT (Table S2).²⁰ Interestingly, in addition to the DAT triplet-derived pattern, the ESR spectrum of DAT-MOF shows a relatively sharp emissive peak around 342 mT, which is derived from radicals (Figure 3b). The time evolution of the ESR spectrum is shown in Figure 3c and 3d. The ESR signal is observed clearly for longer times in the radicals when compared to the triplets. The decay curve at 375 mT, the absorption peak of triplet, shows that the time constant of decay is 0.81 μs . The emissive peak of radical at 342 mT rises with a time constant of 0.85 μs , which is comparable to the time constant of decay of triplet. This implies that polarization transfers from triplets to already generated radicals, or to radicals generated by charge separation from triplets.

In order to determine T_1 we performed pulsed ESR measurements. By an inversion recovery sequence (Figure 3e) at the emissive peak of the radicals (343 mT) at room temperature, T_1 of radical in DAT-MOF was found to be as long as 274 μs (Figure 3f). This extremely long T_1 even at room temperature may be attributed to DAT moieties not forming strong interactions with each other and that those molecular motions are suppressed by π - π interactions with BPDC. A more detailed mechanism would require further investigation by systematically changing the MOF structure.

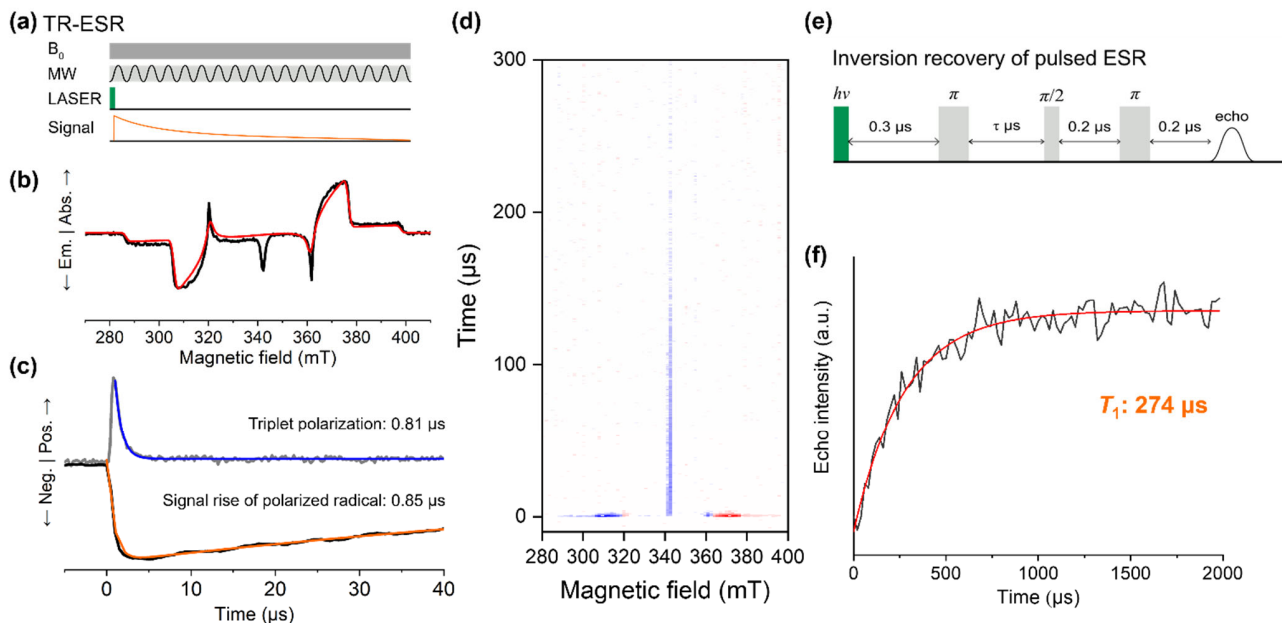


Figure 3. (a) Sequence of time-resolved ESR measurement. (b) Time-resolved ESR (TR-ESR) spectrum of DAT-MOF at room temperature just after photoexcitation at 532 nm (black line). The simulated spectrum is also shown (red line). Fitting parameters are summarized in Table S2. (c) Decays of the TR-ESR peaks of triplet at 374 mT (gray line) and of radical at 343 mT (black line) in DAT-MOF at room temperature. Single-exponential fitting curve for triplet (blue line) and double-exponential fitting curve for radical (orange line) are also shown. (d) The 2D time-resolved ESR spectrum in terms of the signal intensity as a function of time delay and magnetic field. (e) Sequence of inversion recovery of pulsed ESR measurements. (f) Decay of echo intensity at 343 mT of pulsed ESR measurements of DAT-MOF at room temperature. Single-exponential fitting curve for the decay signal is also shown (red line).

To confirm that the emissive peak at 343 mT is of radical origin, Rabi nutation experiments²⁵ were performed on the triplet and radical peaks (Figure 4a). The Rabi nutation frequency Ω at the transition between two spin sublevels, m_s and $m_s \pm 1$, is given by the following equation,

$$\Omega = \omega_1 \sqrt{S(S+1) - m_s(m_s \pm 1)}$$

where $\omega_1 = g\mu_B B_1 / \hbar$ and g, μ_B, B_1 , and \hbar are g factor, Bohr magneton, ac magnetic field strength, and reduced Planck constant, respectively. The Rabi frequency should be $\sqrt{2}$ times larger for the $m_s = 0 \rightarrow m_s = -1$ transition of the triplet ($S = 1$) than for the $m_s = 1/2 \rightarrow m_s = -1/2$ transition of the radical ($S = 1/2$). The Fourier transform of the observed Rabi oscillations at the same external microwave intensity shows that the triplet and radical peaks are at 18 MHz and 12 MHz respectively, and their ratio is close to a factor of $\sqrt{2}$ (Figure 4b). This result proves that the emissive peak at 343 mT is indeed due to radicals.

Next, to gain a better understanding of what kind of radical was formed, continuous-wave (cw) ESR measurements with magnetic field modulation were performed after irradiating with and then stopping the laser (Figure 4c). The obtained g value of 2.0023 is typical for aromatic radicals,²⁶ and the shape of the spectrum suggested that the radicals were those of the oxidized/reduced acene molecules formed by charge separation. The differential cw-ESR spectrum was converted to the integral form, and the peak shape is in good agreement with that of the time-resolved ESR spectrum, indicating that the same radical species was polarized immediately after the photoexcita-

tion (Figure S4). The gradual increase in the intensity of the radical peak was observed during continuous laser irradiation of DAT-MOF (Figure 4d). Interestingly, even a few hours after stopping photoirradiation, the radical peak remained, indicating that radicals generated in DAT-MOF are persistent.

The formation of radicals of the DPyDAT ligand was further verified by optical spectroscopy. Since it takes many hours for the persistent radicals to disappear, the changes cannot be followed by ordinary transient absorption measurements. Therefore, we measured the absorption spectra of DAT-MOF immediately after and after 12 h of continuous laser irradiation for 20 minutes. The pristine DAT-MOF without photoexcitation showed a ligand-derived absorption band below 600 nm (Figure S5). On the other hand, DAT-MOF immediately after laser irradiation showed a new broad absorption band between 600-900 nm, and its intensity decreased after 12 h in the dark (Figure 4e). To investigate the origin of this new absorption band, DAT-MOF was chemically oxidized in a CH_2Cl_2 solution of SbCl_5 . SbCl_5 has been used as an oxidant to produce cation radical of acene compounds.²⁷ Chemically-oxidized DAT-MOF showed a new absorption around 600-800 nm (Figure 4f). The fact that the similar absorption band was observed when only the ligand DPyDAT was oxidized with SbCl_5 in CH_2Cl_2 suggests that the absorption band between 600-800 nm is due to the cation radical of DPyDAT generated in DAT-MOF (Figure S6). Therefore, it is likely that DPyDAT cation radicals are also generated by photoirradiation of DAT-MOF. The reason for the slight difference in absorption spectra between photoirradiation and chemical

oxidation of DAT-MOF is not clear, but the type of reduced products is certainly different.

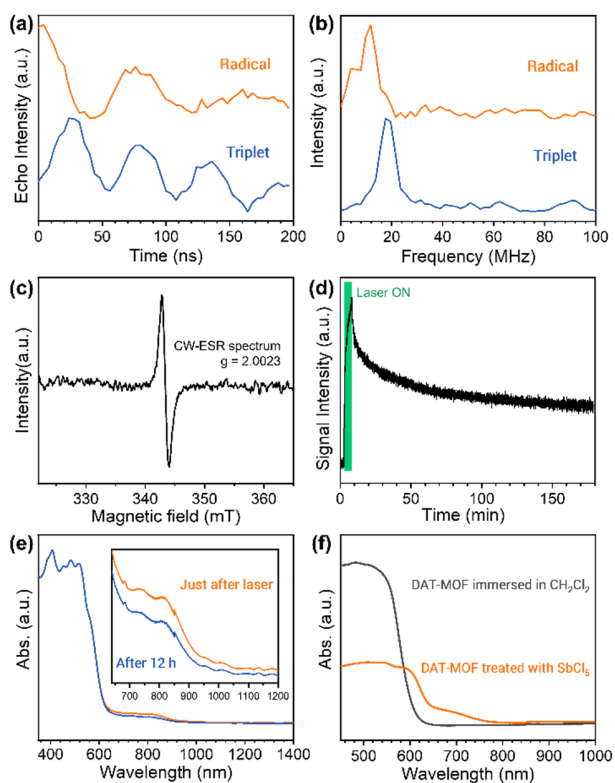


Figure 4. (a) Echo intensity measured as a function of microwave pulse length (Rabi oscillations) at 342 mT and 375 mT for radical (orange line) and triplet (blue line), respectively, of DAT-MOF at room temperature just after photoexcitation at 532 nm. (b) Fourier transform of Rabi oscillations in (a). (c) Continuous wave (cw) ESR spectrum of DAT-MOF at room temperature. (d) Time dependence of cw-ESR signal intensity of DAT-MOF at 342 mT during and after the laser irradiation for 20 min. Pulsed laser irradiation with wavelength, frequency, and power of 532 nm, 30 Hz, and 2 mJ/pulse were used, respectively. (e) UV-Vis absorption spectra of DAT-MOF immediately (orange line) and 12 hours after (blue line) light irradiation. Pulsed laser irradiation with wavelength, frequency, and power of 532 nm, 10 Hz, and 76 mW were used, respectively. (f) UV-Vis absorption spectra of DAT-MOF chemically oxidized by SbCl_5 in CH_2Cl_2 solution (orange line) and just immersed CH_2Cl_2 for comparison (black line).

The measurements described so far were performed without removing the guest water molecules in DAT-MOF. To investigate whether the presence of guest water molecules is essential for radical formation, ESR spectra were measured after removing the guest water molecules. According to the thermogravimetric analysis (TGA), water molecules should be removed below 100 °C (Figure S7). By heating DAT-MOF at 100 °C under vacuum, guest water molecules were completely removed, as demonstrated by the TGA curve. The guest-removed DAT-MOF was similarly immersed in paraffin and its transient ESR spectra were measured. Similar transient ESR spectra were observed for DAT-MOF after removing guest water molecules (Figure S8). Although a radical-derived ESR peak was observed for the heat-evacuated sample, its intensity was weaker and the signal-to-noise ratio was lower (Figure S9). The broadened PXRD pattern of the heat-evacuated DAT-MOF indicates that the removal of guest water molecule re-

duced the crystallinity (Figure S10). These results suggest that the presence of water molecules as guests is not essential for polarized radical formation and that the MOF crystallinity may affect polarized radical formation. In DAT-MOF, the short axes of the DAT moieties were all oriented in the same direction. Even if triplets hopped between the DAT units, the orientation of the DAT moieties in relation to the magnetic field did not change significantly, and the deactivation of triplet polarization may be suppressed.²⁸ The polarization of triplets should be more easily lost when the crystallinity deteriorates and the orientation of DAT is disrupted, which would decrease the efficiency of polarization generation of radicals. In other words, it suggests that aligning chromophores in one direction is a useful design for generation of radical polarization.

In conclusion, we have succeeded in generating polarization of radicals with an extremely long spin-lattice relaxation time, T_1 , of 274 μs at room temperature in a MOF with densely integrated DAT chromophores. Upon photoexcitation, persistent ligand radicals were generated in the DAT-MOF and a triplet-to-radical polarization transfer occurred. It is implied that the generation of extremely long polarization is achieved by weakening the interaction between the chromophores, while at the same time suppressing their mobility through interaction with the surrounding molecules (in the current case, BPDC co-ligand). It also seems important to orient the chromophores in one direction so that the polarization of the triplet, the source of the polarization, does not relax immediately. Future studies that systematically vary the chromophores and their assembly structures will provide a better understanding of the generation of super-long-lived radical polarization. The combination of long-lived polarization and accessible nanospace is expected to lead to unique applications such as highly sensitive quantum sensing of guest chemicals and nuclear spin polarization of guest biomolecules.

ASSOCIATED CONTENT

Supporting Information. Experimental details, synthesis and characterization of DPyDAT and DAT-MOF, PXRD patterns, time-resolved ESR data, UV-Vis absorption spectra, TGA curves.

AUTHOR INFORMATION

Corresponding Author

*yanai@mail.cstm.kyushu-u.ac.jp

Notes

The authors declare no competing financial interests.

ACKNOWLEDGMENT

This work was partly supported by the JST-FOREST Program (JPMJFR201Y) and JSPS KAKENHI (JP20H02713, JP20K21211, JP22K19051, and JP21J21996), JST SPRING (JPMJSP2136), The Murata Science Foundation, Research Foundation for Opto-Science and Technology, Kyushu University Platform of Inter-/Transdisciplinary Energy Research (Q-PIT) through its "Module-Research Program", the RIKEN-Kyushu University of Science and Technology Hub Collaborative Research Program, and the RIKEN Cluster for Science, Technology and Innovation Hub (RCSTI). Part of this work was conducted at Institute for Molecular Science, supported by Advanced Research Infrastructure for Materials and Nanotechnology (JPMXP1222MS0010), and by Nanotechnology Platform Pro-

gram <Molecule and Material Synthesis> (JPMXP09S21MS0038), of the Ministry of Education, Culture, Sports, Science and Technology (MEXT), Japan.

REFERENCES

- (1) Atzori, M.; Sessoli, R. The Second Quantum Revolution: Role and Challenges of Molecular Chemistry. *J. Am. Chem. Soc.* **2019**, *141*, 11339–11352.
- (2) Yu, C.-J.; von Kugelgen, S.; Laorenza, D. W.; Freedman, D. E. A Molecular Approach to Quantum Sensing. *ACS Cent. Sci.* **2021**, *7*, 712–723.
- (3) Wasielewski, M. R.; Forbes, M. D. E.; Frank, N. L.; Kowalski, K.; Scholes, G. D.; Yuen-Zhou, J.; Baldo, M. A.; Freedman, D. E.; Goldsmith, R. H.; Goodson, T.; Kirk, M. L.; McCusker, J. K.; Ogilvie, J. P.; Shultz, D. A.; Stoll, S.; Whaley, K. B. Exploiting Chemistry and Molecular Systems for Quantum Information Science. *Nat. Rev. Chem.* **2020**, *4*, 490–504.
- (4) Overhauser, A. W. Polarization of Nuclei in Metals. *Phys. Rev.* **1953**, *92*, 411–415.
- (5) Carver, T. R.; Slichter, C. P. Polarization of Nuclear Spins in Metals. *Phys. Rev.* **1953**, *92*, 212–213.
- (6) Ardenkjaer-Larsen, J. H.; Fridlund, B.; Gram, A.; Hansson, G.; Hansson, L.; Lerche, M. H.; Servin, R.; Thaning, M.; Golman, K. Increase in Signal-to-Noise Ratio of > 10,000 Times in Liquid-State NMR. *Proc. Natl. Acad. Sci. U. S. A.* **2003**, *100*, 10158–10163.
- (7) Nishimura, K.; Kouno, H.; Kawashima, Y.; Orihashi, K.; Fujiwara, S.; Tateishi, K.; Uesaka, T.; Kimizuka, N.; Yanai, N. Materials Chemistry of Triplet Dynamic Nuclear Polarization. *Chem. Commun.* **2020**, *56*, 7217–7232.
- (8) Eills, J.; Budker, D.; Cavagnero, S.; Chekmenev, E. Y.; Elliott, S. J.; Jannin, S.; Lesage, A.; Matysik, J.; Meersmann, T.; Prisner, T.; Reimer, J. A.; Yang, H.; Koptiyug, I. V. Spin Hyperpolarization in Modern Magnetic Resonance. *Chem. Rev.* **2023**, *123*, 1417–1551.
- (9) Yamabayashi, T.; Atzori, M.; Tesi, L.; Cosquer, G.; Santanni, F.; Boulon, M.-E.; Morra, E.; Benci, S.; Torre, R.; Chiesa, M.; Sorace, L.; Sessoli, R.; Yamashita, M. Scaling Up Electronic Spin Qubits into a Three-Dimensional Metal-Organic Framework. *J. Am. Chem. Soc.* **2018**, *140*, 12090–12101.
- (10) Laorenza, D. W.; Kairalapova, A.; Bayliss, S. L.; Goldzak, T.; Greene, S. M.; Weiss, L. R.; Deb, P.; Mintun, P. J.; Collins, K. A.; Awschalom, D. D.; Berkelbach, T. C.; Freedman, D. E. Tunable Cr⁴⁺ Molecular Color Centers. *J. Am. Chem. Soc.* **2021**, *143*, 21350–21363.
- (11) Harvey, S. M.; Wasielewski, M. R. Photogenerated Spin-Correlated Radical Pairs: From Photosynthetic Energy Transduction to Quantum Information Science. *J. Am. Chem. Soc.* **2021**, *143*, 15508–15529.
- (12) Kothe, G.; Lukaschek, M.; Yago, T.; Link, G.; Ivanov, K. L.; Lin, T.-S. Initializing 214 Pure 14-Qubit Entangled Nuclear Spin States in a Hyperpolarized Molecular Solid. *J. Phys. Chem. Lett.* **2021**, *12*, 3647–3654.
- (13) Kirk, M. L.; Shultz, D. A.; Hewitt, P.; Stasiw, D. E.; Chen, J.; van der Est, A. Chromophore-Radical Excited State Antiferromagnetic Exchange Controls the Sign of Photoinduced Ground State Spin Polarization. *Chem. Sci.* **2021**, *12*, 13704–13710.
- (14) Mayländer, M.; Chen, S.; Lorenzo, E. R.; Wasielewski, M. R.; Richert, S. Exploring Photogenerated Molecular Quartet States as Spin Qubits and Qudits. *J. Am. Chem. Soc.* **2021**, *143*, 7050–7058.
- (15) Paquette, M. M.; Plaul, D.; Kurimoto, A.; Patrick, B. O.; Frank, N. L. Opto-Spintronics: Photoisomerization-Induced Spin State Switching at 300 K in Photochrome Cobalt-Dioxolene Thin Films. *J. Am. Chem. Soc.* **2018**, *140*, 14990–15000.
- (16) Bayliss, S. L.; Laorenza, D. W.; Mintun, P. J.; Kovos, B. D.; Freedman, D. E.; Awschalom, D. D. Optically Addressable Molecular Spins for Quantum Information Processing. *Science* **2020**, *370*, 1309–1312.
- (17) Jackson, C. E.; Moseley, I. P.; Martinez, R.; Sung, S.; Zadrozny, J. M. A Reaction-Coordinate Perspective of Magnetic Relaxation. *Chem. Soc. Rev.* **2021**, *50*, 6684–6699.
- (18) Kirk, M. L.; Shultz, D. A.; Hewitt, P.; van der Est, A. Excited State Exchange Control of Photoinduced Electron Spin Polarization in Electronic Ground States. *J. Phys. Chem. Lett.* **2022**, *13*, 872–878.
- (19) Oanta, A. K.; Collins, K. A.; Evans, A. M.; Pratik, S. M.; Hall, L. A.; Strauss, M. J.; Marder, S. R.; D'Alessandro, D. M.; Rajh, T.; Freedman, D. E.; Li, H.; Brédas, J.-L.; Sun, L.; Dichtel, W. R. Electronic Spin Qubit Candidates Arrayed within Layered Two-Dimensional Polymers. *J. Am. Chem. Soc.* **2023**, *145*, 689–696.
- (20) Kouno, H.; Kawashima, Y.; Tateishi, K.; Uesaka, T.; Kimizuka, N.; Yanai, N. Nonpentacene Polarizing Agents with Improved Air Stability for Triplet Dynamic Nuclear Polarization at Room Temperature. *J. Phys. Chem. Lett.* **2019**, *10*, 2208–2213.
- (21) Kouno, H.; Orihashi, K.; Nishimura, K.; Kawashima, Y.; Tateishi, K.; Uesaka, T.; Kimizuka, N.; Yanai, N. Triplet Dynamic Nuclear Polarization of Crystalline Ice Using Water-Soluble Polarizing Agents. *Chem. Commun.* **2020**, *56*, 3717–3720.
- (22) Fujiwara, S.; Matsumoto, N.; Nishimura, K.; Kimizuka, N.; Tateishi, K.; Uesaka, T.; Yanai, N. Triplet Dynamic Nuclear Polarization of Guest Molecules through Induced Fit in a Flexible Metal-Organic Framework. *Angew. Chem. Int. Ed Engl.* **2022**, *61*, e202115792.
- (23) Uemura, K.; Yamasaki, Y.; Komagawa, Y.; Tanaka, K.; Kita, H. Two-step adsorption/desorption on a jungle-gym-type porous coordination polymer. *Angew. Chem. Weinheim Bergstr. Ger.* **2007**, *119*, 6782–6785.
- (24) Chen, B.; Liang, C.; Yang, J.; Contreras, D. S.; Clancy, Y. L.; Lobkovsky, E. B.; Yaghi, O. M.; Dai, S. A Microporous Metal-Organic Framework for Gas-Chromatographic Separation of Alkanes. *Angew. Chem. Int. Ed Engl.* **2006**, *45*, 1390–1393.
- (25) Astashkin, A. V.; Schweiger, A. Electron-Spin Transient Nutation: A New Approach to Simplify the Interpretation of ESR Spectra. *Chem. Phys. Lett.* **1990**, *174*, 595–602.
- (26) Li, Q.; Zhang, Q.; Wei, W.-J.; Wang, A.-N.; Hu, J.-X.; Wang, G.-M. Light Actuated Stable Radicals of the 9-Anthracene Carboxylic Acid for Designing New Photochromic Complexes. *Chem. Commun.* **2021**, *57*, 4295–4298.
- (27) Uebe, M.; Kawashima, K.; Takahashi, K.; Ito, A. Mesityl-Substituted Acene Radical Cations: Decent Stability Comparable to Their Neutral States under Ambient Light and Air. *Chemistry* **2017**, *23*, 278–281.
- (28) Jaegermann, P.; Plato, M.; von Maltzan, B.; Möbius, K. Time-Resolved EPR Study of Exciton Hopping in Porphyrin Dimers in Their Photoexcited Triplet State. *Mol. Phys.* **1993**, *78*, 1057–1074.